



## Open Archive Toulouse Archive Ouverte






OATAO is an open access repository that collects the work of Toulouse researchers and makes it freely available over the web where possible

This is an author's version published in: <http://oatao.univ-toulouse.fr/20948>

### Official URL:

<http://dx.doi.org/10.1021/acs.est.5b06058>

### To cite this version:

Enrico, Maxime  and Le Roux, Gaël  and Maruszczak, Nicolas  and Heimbürger, Lars-Éric  and Claustres, Adrien and Fu, Xuewu and Sun, Ruoyu  and Sonke, Jeroen E. *Atmospheric Mercury Transfer to Peat Bogs Dominated by Gaseous Elemental Mercury Dry Deposition*. (2016) *Environmental Science & Technology*, 50 (5). 2405-2412. ISSN 0013-936X

Any correspondence concerning this service should be sent to the repository administrator: [tech-oatao@listes-diff.inp-toulouse.fr](mailto:tech-oatao@listes-diff.inp-toulouse.fr)

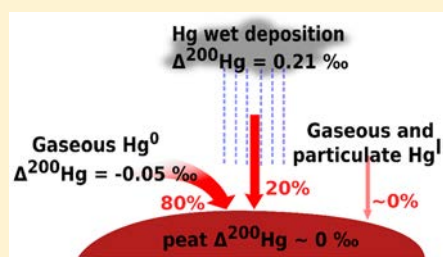
# Atmospheric Mercury Transfer to Peat Bogs Dominated by Gaseous Elemental Mercury Dry Deposition

Maxime Enrico,<sup>\*,†,‡</sup> Gaël Le Roux,<sup>†</sup> Nicolas Maruszczak,<sup>‡</sup> Lars-Eric Heimbürger,<sup>‡,§</sup> Adrien Claustres,<sup>†</sup> Xuewu Fu,<sup>‡,⊥</sup> Ruoyu Sun,<sup>‡,#</sup> and Jeroen E. Sonke<sup>\*,‡</sup>

<sup>†</sup>ECOLAB, Université de Toulouse, CNRS, INPT, UPS, France; ENSAT, Avenue de l'Agrobiopole, 31326 Castanet Tolosan, France

<sup>‡</sup>Observatoire Midi-Pyrénées, Laboratoire Géosciences Environnement Toulouse, CNRS/IRD/Université Paul Sabatier Toulouse III, 14 avenue Edouard Belin, 31400 Toulouse, France

**ABSTRACT:** Gaseous elemental mercury (GEM) is the dominant form of mercury in the atmosphere. Its conversion into oxidized gaseous and particulate forms is thought to drive atmospheric mercury wet deposition to terrestrial and aquatic ecosystems, where it can be subsequently transformed into toxic methylmercury. The contribution of mercury dry deposition is however largely unconstrained. Here we examine mercury mass balance and mercury stable isotope composition in a peat bog ecosystem. We find that isotope signatures of living sphagnum moss ( $\Delta^{199}\text{Hg} = -0.11 \pm 0.09\text{‰}$ ,  $\Delta^{200}\text{Hg} = 0.03 \pm 0.02\text{‰}$ ,  $1\sigma$ ) and recently accumulated peat ( $\Delta^{199}\text{Hg} = -0.22 \pm 0.06\text{‰}$ ,  $\Delta^{200}\text{Hg} = 0.00 \pm 0.04\text{‰}$ ,  $1\sigma$ ) are characteristic of GEM ( $\Delta^{199}\text{Hg} = -0.17 \pm 0.07\text{‰}$ ,  $\Delta^{200}\text{Hg} = -0.05 \pm 0.02\text{‰}$ ,  $1\sigma$ ), and differs from wet deposition ( $\Delta^{199}\text{Hg} = 0.73 \pm 0.15\text{‰}$ ,  $\Delta^{200}\text{Hg} = 0.21 \pm 0.04\text{‰}$ ,  $1\sigma$ ). Sphagnum covered during three years by transparent and opaque surfaces, which eliminate wet deposition, continue to accumulate Hg. Sphagnum Hg isotope signatures indicate accumulation to take place by GEM dry deposition, and indicate little photochemical re-emission. We estimate that atmospheric mercury deposition to the peat bog surface is dominated by GEM dry deposition (79%) rather than wet deposition (21%). Consequently, peat deposits are potential records of past atmospheric GEM concentrations and isotopic composition.



## INTRODUCTION

Mercury (Hg) is a toxic element to humans and wildlife, especially in its methylated forms.<sup>1</sup> Modern anthropogenic Hg emissions ( $\sim 2000 \text{ Mg y}^{-1}$ )<sup>2</sup> outweigh natural volcanic emissions ( $76\text{--}300 \text{ Mg y}^{-1}$ )<sup>3,4</sup> by an order of magnitude.<sup>5</sup> Gaseous elemental mercury (GEM), the dominant Hg form in the atmospheric boundary layer, is relatively unreactive, leading to a long atmospheric lifetime of 6–12 months and wide dispersal of GEM across the globe.<sup>6</sup> Atmospheric GEM can be oxidized to soluble and short-lived gaseous oxidized Hg (GOM) species that may adsorb to aerosols to form particulate bound Hg (PBM). GOM and PBM are readily transferred back to the Earth's surface via wet (i.e., rain and snow fall) and dry deposition, thereby providing substrate to microbial Hg methylation in aquatic ecosystems.<sup>7,8</sup> Dry deposition includes foliar uptake of GEM and GOM, surface sorption of GEM and GOM to vegetation and soil, dissolution of GEM and GOM in water bodies, and gravitational deposition of PBM.<sup>7</sup> Wet deposition of Hg is well-constrained relative to dry deposition, yet occurs only 2–5% of the time in terms of meteorological conditions globally, while dry deposition occurs almost continuously (95–98% of the time).<sup>7</sup> Dry deposition of GOM, PBM and in particular GEM is notoriously difficult to assess because it occurs at slow rates, and is a net balance between dry deposition and re-emission from soil and vegetation surfaces.<sup>8,9</sup> Diverse field studies have investigated

GEM transfer between atmosphere and continents and find evidence for both net GEM dry deposition or net GEM emission depending on factors such as light radiation (seasonal and diurnal cycles), temperature, GEM concentration and canopy wetness.<sup>10–15</sup> While GEM dry deposition has been suggested to be significant in the global Hg mass balance,<sup>16</sup> the variability in GEM dynamics complicates the determination of a net annual balance ( $-513$  to  $+1353 \text{ Mg a}^{-1}$  uncertainty range).<sup>17</sup>

Mercury's seven stable isotopes fractionate both mass dependently (MDF) and mass independently (MIF) during partial Hg transformations and Hg source mixing. This gives rise to five useful isotope signatures,  $\delta^{202}\text{Hg}$ ,  $\Delta^{199}\text{Hg}$ ,  $\Delta^{201}\text{Hg}$ ,  $\Delta^{200}\text{Hg}$ , and  $\Delta^{204}\text{Hg}$ , that reflect different Hg sources and/or processes.<sup>18,19</sup> All investigated biogeochemical Hg transformations display mass dependent Hg isotope fractionation (MDF, represented by  $\delta^{202}\text{Hg}$ ).<sup>19</sup> Large odd Hg isotope mass independent fractionation (MIF,  $\Delta^{199}\text{Hg}$ ,  $\Delta^{201}\text{Hg}$ ) is predominantly photochemical in origin<sup>20</sup> with a minor and unclear role for nuclear field shift effects.<sup>21,22</sup> The mechanism of even isotope Hg MIF ( $\Delta^{200}\text{Hg}$ ,  $\Delta^{204}\text{Hg}$ ), which is characteristic of

rainfall Hg<sup>23,24</sup> is not understood. Absence of even isotope MIF during biogeochemical Hg transformations at the Earth's surface<sup>19</sup> and the observation of large positive  $\Delta^{200}\text{Hg}$  in precipitation from air masses with an upper atmospheric origin has led to the idea of an upper atmospheric (tropopause, i.e. boundary between troposphere and stratosphere at 5–10 km altitude) origin for  $\Delta^{200}\text{Hg}$ .<sup>24</sup>

The objective of this study was to investigate the dominant Hg deposition processes to peat bogs. We therefore examine Hg deposition fluxes and Hg stable isotope signatures of wet deposition, atmospheric GEM and reactive Hg (combined GOM+PBM) fractions, sphagnum mosses and peat in a peat bog ecosystem in the French Pyrenees and at the upwind Pic du Midi Observatory.

## EXPERIMENTAL SECTION

**Sampling Sites.** The Pinet peat bog (42°52' N, 1° 58' E) is located in the French Pyrenees at 880 m elevation (Figure 1).



**Figure 1.** Location of the sampling sites (Google Earth image): the Pinet peat bog and the Pic du Midi observatory (A), and picture of the experimental set up on the Pinet peat bog (B).

The surface of the peat bog is presently covered by sphagnum, calluna and pines. Annual precipitation in the area is 1161 mm (average for the period 2010–2013). The Pinet bog is 5 m deep, representing 10 000 years of peat accumulation.

The Pic du Midi observatory (42.94° N, 0.14° E) is located in the French Pyrenees at 2877 m elevation (Figure 1). Atmospheric Hg concentration (GEM, GOM, and PBM) is monitored at this site using a Tekran 2537/1130/1135 system.<sup>25</sup>

**Peat Sampling.** Three peat cores were sampled in September 2010 at the Pinet peat bog using a Wardenaar corer. The upper 20 cm peat profiles are presented and compared to fresh *Sphagnum* samples from the same sites (upper 25 cm for core C). Frozen peat cores were sliced into 1 cm layers, and one-quarter of each slice was dedicated to Hg concentration and isotope measurements. The three peat cores were measured for <sup>210</sup>Pb, <sup>137</sup>Cs and <sup>241</sup>Am activities by Gamma-spectrometry and dated assuming a constant rate of supply of <sup>210</sup>Pb (see Supporting Information (SI), Figure S1). Dry bulk density was determined in all peat layers to allow the calculation of peat accumulation rate (in g m<sup>-2</sup> y<sup>-1</sup>).

**Rain Water Sampling.** During the summer of 2014 (July 10th to August 19th), thirteen 40 cm diameter polypropylene buckets were installed on top of the opaque covers in order to collect event based wet precipitation samples. To avoid any loss of Hg by photochemistry, rain samples were recovered within 3 h following each rain event. Rain samples were transferred into precleaned Pyrex glass bottles (1 and 2 L volume). Each bucket was rinsed with MQ water between all sampling events.

All rain samples were then oxidized by adding 0.1–1% BrCl until the samples remained slightly yellow (BrCl in excess), and kept refrigerated before processing.

**Air Sampling.** Gaseous elemental mercury (GEM) was sampled at the Pinet site during the same period by pumping air through iodated carbon traps.<sup>25</sup> Two pumps were installed in parallel 20 cm above the bog surface, with flow rates of approximately 1.5 and 2.5 L·min<sup>-1</sup>. One of the iodated carbon traps was preceded by a quartz filter. A polyethersulfone cation exchange membrane (CEM) filter (Sterlitech, 0.45 μm pore size, 47 mm diameter) preceded the parallel iodated carbon trap to allow determination of gaseous oxidized mercury (GOM) plus particulate bound mercury (PBM) concentrations, following protocols by Huang et al.<sup>26</sup> An air volume of 91 m<sup>3</sup> was sampled through the CEM at Pinet site. Iodated carbon traps were changed every 6–8 days, and we collected a total of 10 GEM samples (five from each pump line). Iodated carbon traps might integrate some GOM as well, especially for those preceded by the quartz filter. However, because of the very low proportion of GOM compared to GEM in the atmospheric boundary layer (<5%),<sup>27</sup> we consider these samples as GEM. Ten additional GEM samples were taken at the Pic du Midi Observatory using chlorinated carbon traps.<sup>25</sup>

**Experimental Design and Sphagnum Sampling.** In December 2011, five experimental plots were installed at the Pinet peat bog: two opaque PVC covers (1 × 1 m, 8 mm thick, no light transmission) and one tempered glass cover (2 × 1 m, 8 mm thick, UV-A and visible wavelengths transmitted) were installed at a height of 30 cm above the peat bog. The covers excluded wet deposition from reaching underlying sphagnum, while ambient air was able to circulate freely. Two 1 m<sup>2</sup> areas left open were used as a control. Sphagnum samples were collected 9 times from December 2011 to July 2014 from designated areas under these plates in all plots. Care was taken to avoid resampling of the same area within a plot over the three-year period. Additionally, Pine needles, *calluna* leaves, and epiphytic lichens were sampled in July 2014 at the same site.

**Hg Concentration Measurements.** Freeze-dried peat, sphagnum, pine needles and *calluna* leaves samples were analyzed for total Hg concentration with a Milestone Direct Mercury Analyzer (DMA 80). The DMA 80 was calibrated using coal (NIST1632d) and lichen (BCR482) CRMs. Accuracy and long-term reproducibility was assessed by replicate measurements of CRMs (NIST1632d, BCR482, and NIMT peat). Results were not statistically different from certified values, with Hg concentrations of 91.6 ± 8.2 ng g<sup>-1</sup> for NIST1632d (1σ, n = 112, certified value 92.8 ± 3.3 ng g<sup>-1</sup>), 472 ± 12 ng g<sup>-1</sup> for BCR482 (1σ, n = 72, certified value 480 ± 20 ng g<sup>-1</sup>) and 158 ± 8 ng g<sup>-1</sup> for NIMT (1σ, n = 22, certified value 164 ± 20 ng g<sup>-1</sup>).

Rain water was analyzed by cold vapor atomic fluorescence spectroscopy (CV-AFS). CV-AFS was calibrated using a diluted NIST3133 solution (0.1 μg L<sup>-1</sup>) and ORMS-5 CRM (certified value 26.2 ± 1.3 ng L<sup>-1</sup>).

The GOM+PBM fraction sampled on the cation exchange membrane filter was dissolved in a 20% inverse *aqua regia* solution. The solution was then also analyzed by CV-AFS. The GOM+PBM sample from the Pinet peat bog, however, was found to be below the method detection limit. This suggests GOM+PBM concentrations below 2.8 pg m<sup>-3</sup> over the Pinet peat bog.

**Sample Procedures for Hg Isotope Measurements.** Hg stable isotopes were measured when sufficient material was

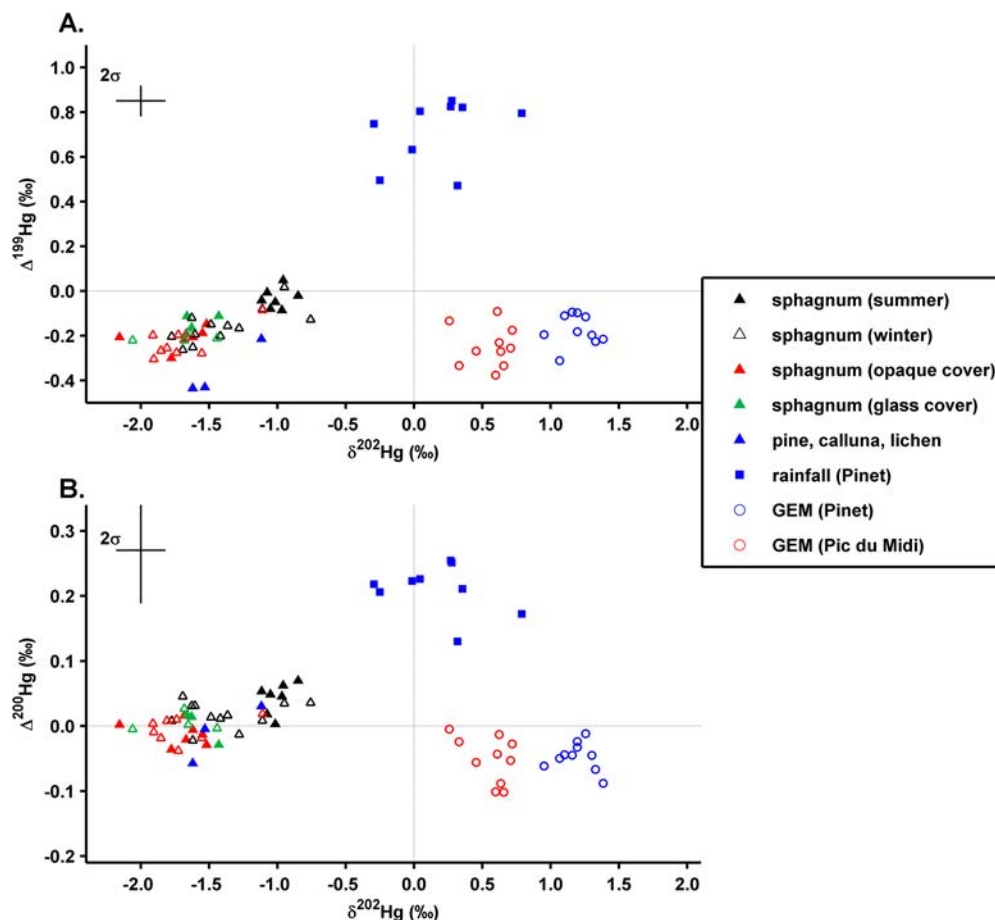


**Figure 2.** Mass dependent ( $\delta^{202}\text{Hg}$ ) and mass-independent Hg isotope signatures of (A) odd (shown as  $\Delta^{199}\text{Hg}$ ) and (B) even Hg isotopes (shown as  $\Delta^{200}\text{Hg}$ ) in atmospheric Hg and sphagnum moss, pine needles, calluna leaves, and lichen (triangles). Sphagnum moss  $\Delta^{199}\text{Hg}$  and  $\Delta^{200}\text{Hg}$  closely resemble GEM, and not Hg wet deposition. The 2.4 per mil depletion of sphagnum  $\delta^{202}\text{Hg}$  compared to GEM reflects foliar uptake of GEM.<sup>39</sup>

available. The first 10 cm of peat core C contained a very low amount of material (<10 ng of Hg per slice) and could not be analyzed for Hg isotopes. Hg was then extracted using a combustion and acid trapping method,<sup>28</sup> with extraction yields in the range 85–110%. An adapted combustion method was used for iodated and chlorinated carbon traps to remove any volatile halogen compounds.<sup>25</sup> Extractions of iodated carbon traps loaded with known amounts of Hg gave yields of  $90 \pm 4\%$  ( $n = 3$ ).

Hg from rainwater was reduced by progressive addition of 100 mL of a 10%  $\text{SnCl}_2$  solution in 1 L samples, purged by bubbling Hg free argon ( $\sim 300 \text{ mL min}^{-1}$ ) and preconcentrated in an oxidizing solution, following the protocol of Sherman et al.<sup>29</sup> Samples consisting of more than 1L were processed in several steps, using the same oxidizing solution. Preconcentration yields were in the range 95–105% ( $n = 9$ ). For both the combustion and the liquid preconcentration methods, we used a 40% (v/v) inverse *aqua regia* ( $\text{HNO}_3/\text{HCl}$ , 2:1) solution as the oxidizing trap solution. Buckets rinsed with mQ water and processed as samples gave blank values below 0.2 ng ( $n = 2$ ), which represents less than 3% of Hg in rainwater samples.

**Hg Isotope Measurements.** Prior to analysis, all solutions were adjusted to an acid concentration of 20% (v/v). Sample solutions were then analyzed for Hg isotope ratios by cold vapor–multicollector inductively coupled plasma mass spectrometry (CV-MC-ICPMS) using a Thermo-Finnigan Neptune at Midi-Pyrenees Observatory (Toulouse, France). Isotopic

ratios were corrected for mass bias by sample bracketing using the international standard NIST SRM 3133.<sup>28</sup> Results are reported as  $\delta$ -values, representing deviation from the bracketing standard and expressed in permil (‰):

$$\delta^{xxx}\text{Hg} = \left( \frac{\left( \frac{xxx\text{Hg}}{^{198}\text{Hg}} \right)_{\text{sample}}}{\left( \frac{xxx\text{Hg}}{^{198}\text{Hg}} \right)_{\text{SRM3133}}} - 1 \right) \times 1000$$

MIF is quantified as the  $\delta$ -values deviation from the theoretical MDF:

$$\Delta^{xxx}\text{Hg} = \delta^{xxx}\text{Hg}_{\text{sample}} - \beta \times \delta^{202}\text{Hg}_{\text{sample}}$$

Where  $\beta$ -values are 0.252, 0.502, 0.752, and 1.493 for isotopes  $^{199}\text{Hg}$ ,  $^{200}\text{Hg}$ ,  $^{201}\text{Hg}$ , and  $^{204}\text{Hg}$  respectively, according to the kinetic MDF law.

Long-term reproducibility of measurements was assessed by analyzing UM-Almaden, ETH-Fluka and the procedural standards (SI Table S1): coal (NIST2685b,  $n = 5$ ), peat (NIMT, NJV942,  $n = 5$  and 3 respectively) and lichen (BCR482,  $n = 6$ ). UM-Almaden displayed  $\delta^{202}\text{Hg}$  and  $\Delta^{199}\text{Hg}$  of  $-0.57 \pm 0.11\%$  and  $-0.04 \pm 0.06\%$  ( $2\sigma$ ,  $n = 46$ ) respectively, and ETH-Fluka had  $\delta^{202}\text{Hg}$  and  $\Delta^{199}\text{Hg}$  of  $-1.43 \pm 0.14\%$  and  $0.08 \pm 0.06\%$  ( $2\sigma$ ,  $n = 57$ ). Reproducibility of the rainwater preconcentration method was assessed by preconcentrating Hg from diluted NIST3133

solutions ( $n = 3$ , initial Hg concentrations of 5, 10, and 15 ng L<sup>-1</sup>). Solutions were then measured for Hg isotope ratios. The variability in the  $\delta$ -values obtained was lower than for procedural coal, peat and lichen SRMs (SI Table S1). Samples were analyzed repeatedly over different session until their long-term reproducibility was the same (or better) as the procedural SRMs. The uncertainties reported in Figure 2 and SI Figures S2–S4 are the highest  $2\sigma$  values on procedural SRMs (SI Table S1), found for NIMT peat SRM (for  $\delta^{202}\text{Hg}$ ,  $\Delta^{200}\text{Hg}$  and  $\Delta^{204}\text{Hg}$ ) and BCR482 (for  $\Delta^{199}\text{Hg}$  and  $\Delta^{201}\text{Hg}$ ).

## RESULTS AND DISCUSSION

**Hg Deposition Mass Balance.** Three <sup>210</sup>Pb dated peat cores from the Pinet peat bog (see SI Figure S1) show a recent net Hg accumulation rate (HgAR) of  $34 \pm 8 \mu\text{g m}^{-2} \text{y}^{-1}$  (mean  $\pm 1\sigma$ , period 2005–2010). Published peat HgARs show similar values globally with median modern HgAR of  $25 \mu\text{g m}^{-2} \text{y}^{-1}$  ( $-4.5, +20, n = 20$ , period 1990–2000).<sup>4</sup> Annual Hg wet deposition at Pinet is  $9.3 \pm 5.3 \mu\text{g m}^{-2} \text{y}^{-1}$  (Table 1) which is

**Table 1. Estimations of Hg Wet Deposition, GOM+PBM and GEM Dry Deposition Compared to Peat HgAR**

Hg wet deposition	c(Hg)	deposition
	ng L <sup>-1</sup>	$\mu\text{g m}^{-2} \text{y}^{-1}$
North America ( $n = 93$ ) <sup>31</sup>		$9.5 \pm 4.2$
Europe ( $n = 13$ ) <sup>30</sup>		$6.8 \pm 3.2$
Pinet	$8.0 \pm 4.6$	$9.3 \pm 5.3^a$
GOM+PBM	pg m <sup>-3</sup>	$\mu\text{g m}^{-2} \text{y}^{-1}$
AMNet ( $n = 9$ ) <sup>34</sup>	4.8 (2.5–14.7)	0.5 (0.1–6.1) <sup>b</sup>
Pinet	< 2.8	< 0.4 <sup>c</sup> (0–6.7)
GEM	ng m <sup>-3</sup>	$\mu\text{g m}^{-2} \text{y}^{-1}$
AMNet ( $n = 9$ ) <sup>34</sup>	$1.4 \pm 0.1$	44 (4–177) <sup>d</sup>
Pinet	$1.2 \pm 0.2$	38 (4–151) <sup>d</sup>
modern peat HgAR		$\mu\text{g m}^{-2} \text{y}^{-1}$
global ( $n = 20$ ) <sup>4</sup>		25 (8–47)
Pinet (2000–2010)		$34 \pm 8$

<sup>a</sup>Calculated using annual precipitation of 1161 mm. <sup>b</sup>Calculated by applying GOM deposition velocity of  $0.93 \text{ cm s}^{-1}$  (range  $0.2\text{--}7.6 \text{ cm s}^{-1}$ ) and PBM deposition velocity of  $0.11 \text{ cm s}^{-1}$  (range  $0.02\text{--}2.1 \text{ cm s}^{-1}$ )<sup>10,35</sup> <sup>c</sup>Calculated considering GOM and PBM accounting for half of GOM+PBM fraction <sup>d</sup>Calculated by applying GEM dry deposition velocity of  $0.1 \text{ cm s}^{-1}$  (range  $0.01\text{--}0.4 \text{ cm s}^{-1}$ )<sup>10</sup>

similar to extensively monitored Hg wet deposition at sites in Europe ( $6.8 \pm 3.2 \mu\text{g m}^{-2} \text{y}^{-1}$ ; annual mean  $\pm 1\sigma$  over 2000–2009)<sup>30</sup> and N-America ( $9.5 \pm 4.2 \mu\text{g m}^{-2} \text{y}^{-1}$ ; annual mean  $\pm 1\sigma$  over 2000–2013).<sup>31</sup> Recent HgAR at the Pinet bog and at Northern hemispheric peat bogs in general is therefore a factor 3 to 4 times higher compared to wet Hg deposition alone.<sup>32</sup> Downward mobilization of <sup>210</sup>Pb has been proposed to explain such elevated HgARs due to an overestimation of peat mass accumulation.<sup>32,33</sup> At Pinet however we observe good correspondence between <sup>210</sup>Pb, <sup>137</sup>Cs, and <sup>241</sup>Am chronologies. The profile of <sup>137</sup>Cs activity in core B shows a maximum in a peat layer corresponding to 1981–1986 deposition (SI Figure S1), consistent with the Chernobyl accident. In the other two cores, no peak in <sup>137</sup>Cs activity was determined. Cores A and C however presented measurable <sup>241</sup>Am activity in layers dated at 1958–1971 (core A) and 1916–1974 (core C), where core A has sufficient resolution to argue for a good correspondence with nuclear weapons testing in the 1960s.

We propose an alternative hypothesis for the elevated HgAR at Pinet and in peat globally by considering a significant contribution from Hg dry deposition to Hg accumulation in peat. The objective here is to test that hypothesis using Hg stable isotopes. For this purpose, we first assume that the calculated HgAR of  $34 \pm 8 \mu\text{g m}^{-2} \text{y}^{-1}$  is not biased by <sup>210</sup>Pb issues, implying that Hg dry deposition to the Pinet peat bog exceeds Hg wet deposition of  $9.3 \pm 5.3 \mu\text{g m}^{-2} \text{y}^{-1}$ . Hg dry deposition is a broad term that includes gravitational PBM deposition, surface sorption of the gas phase GOM and GOM forms and foliar uptake of GEM by stomata and porous cell walls.

We measured GOM+PBM concentrations at Pinet. Manual GOM+PBM sampling using cation exchange membranes<sup>26</sup> indicated GOM+PBM to be below the method detection limit ( $<2.8 \text{ pg m}^{-3}$ ), defined as three times the standard deviation of the cation exchange filter blank and taking into account the 93 m<sup>3</sup> of filtered air. Low GOM+PBM levels  $<2.8 \text{ pg m}^{-3}$  are typical of continental, forested sites, for example, median North American levels of GOM and PBM are 1.2 and 2.9 pg m<sup>-3</sup>.<sup>34</sup> Observations of GOM and PBM dry deposition velocities over vegetation show a large variability ( $0.2\text{--}7.6 \text{ cm s}^{-1}$  for GOM and  $0.02\text{--}2.1 \text{ cm s}^{-1}$  for PBM).<sup>10</sup> Model based (GEOS-Chem) estimates of global GOM and PBM dry deposition velocities fall in the midrange of observations, that is, 0.93 and 0.11 cm s<sup>-1</sup> for GOM and PBM respectively.<sup>35</sup> Based on this range of dry deposition velocities and our detection limit, we estimate dry deposition of GOM + PBM to the Pinet bog to be in the range of 0 to  $7 \mu\text{g m}^{-2} \text{y}^{-1}$ , and most likely around  $0.4 \mu\text{g m}^{-2} \text{y}^{-1}$  (assuming that GOM and PBM both account for half of the GOM+PBM fraction and using model based deposition velocities, Table 1). The most likely dominant deposition pathway is therefore GEM dry deposition to peat surface vegetation, by foliar uptake, which has been shown previously to be capable of exceeding Hg wet deposition in vegetated ecosystems<sup>36–38</sup> (Table 1).

**Hg Isotope Composition of Sphagnum and Atmospheric Hg.** We first examined the Hg isotope composition of atmospheric GEM, and Hg wet deposition at Pinet and 150 km upwind at Pic du Midi Observatory. Figure 2 and SI Figure S2 show that GEM and Hg wet deposition have substantially different  $\delta^{202}\text{Hg}$ ,  $\Delta^{199}\text{Hg}$  (and  $\Delta^{201}\text{Hg}$ ), and  $\Delta^{200}\text{Hg}$  (and  $\Delta^{204}\text{Hg}$ ). Odd Hg isotope anomalies are found to be positive in wet deposition ( $\Delta^{199}\text{Hg} = 0.72 \pm 0.15\text{‰}$ ,  $1\sigma$ ,  $n = 9$ ), and slightly negative in GEM ( $\Delta^{199}\text{Hg} = -0.17 \pm 0.07\text{‰}$  at Pinet and  $-0.25 \pm 0.09\text{‰}$  at the Pic du Midi,  $1\sigma$ ,  $n = 10$  for both). Even Hg isotope anomalies also indicate a difference between wet deposition ( $\Delta^{200}\text{Hg} = 0.21 \pm 0.04\text{‰}$ ,  $1\sigma$ ,  $n = 9$ ) and GEM ( $\Delta^{200}\text{Hg} = -0.05 \pm 0.02\text{‰}$  at Pinet and  $-0.05 \pm 0.04\text{‰}$  at the Pic du Midi,  $1\sigma$ ,  $n = 10$  for both). These observations are broadly in agreement with global GEM isotopic observations (negative  $\Delta^{199}\text{Hg}$ , close to zero  $\Delta^{200}\text{Hg}$  and  $\Delta^{204}\text{Hg}$ )<sup>23,25,39,40</sup> and rainfall Hg (positive  $\Delta^{199}\text{Hg}$ , positive  $\Delta^{200}\text{Hg}$ , negative  $\Delta^{204}\text{Hg}$ )<sup>23,24,39,41</sup>. The frequently reported positive anomalies in  $\Delta^{200}\text{Hg}$  are thought to originate from the upper atmosphere during the oxidation of GEM.<sup>24</sup> As observed by Demers et al.,<sup>39</sup> we find that  $\Delta^{200}\text{Hg}$  and  $\Delta^{204}\text{Hg}$  are inversely correlated (SI Figure S3), suggesting that they are both generated by the same process.

Living sphagnum moss has similar  $\Delta^{199}\text{Hg}$ ,  $\Delta^{200}\text{Hg}$ ,  $\Delta^{201}\text{Hg}$  and  $\Delta^{204}\text{Hg}$  as GEM (Figure 2, SI Table S2). Sphagnum  $\delta^{202}\text{Hg}$  is however  $-2.4\text{‰}$  lower than GEM  $\delta^{202}\text{Hg}$  of  $1.2 \pm 0.1\text{‰}$  ( $1\sigma$ ,  $n = 10$ ). Pooled samples of pine needles, *Calluna* (heather)

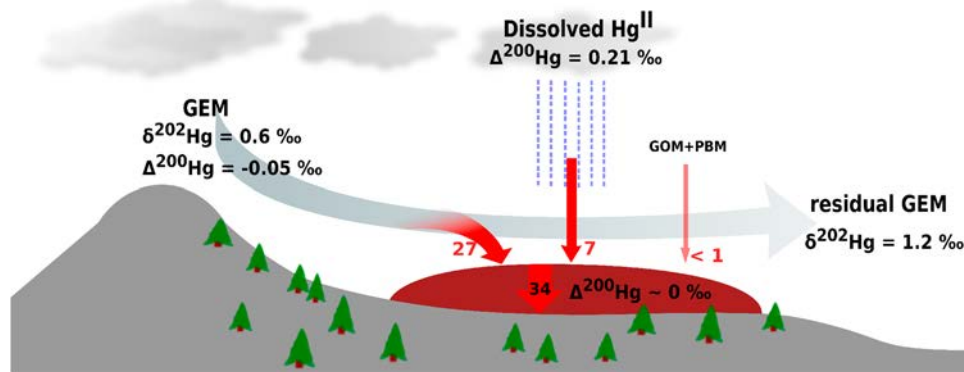


**Figure 3.** Summary of atmospheric Hg inputs into the Pinet peat bog. A  $\Delta^{200}\text{Hg}$ -based mass balance suggests that GEM dry deposition outweighs Hg wet deposition to sphagnum moss by 4-fold. Red numbers indicate net Hg fluxes to the peat bog in  $\mu\text{g m}^{-2} \text{y}^{-1}$ . Regional background GEM levels and  $\delta^{202}\text{Hg}$  at the Pic du Midi suggest that vegetation draws down substantial amounts of atmospheric GEM.

leaves and epiphytic lichens at Pinet show similar shifts of  $-2.3$  to  $-2.8\%$  in  $\delta^{202}\text{Hg}$  (Figure 2). In the first exhaustive Hg stable isotope study of a forest ecosystem, Demers et al.<sup>39</sup> already observed that foliar uptake of atmospheric Hg by aspen trees induces a large ( $-2.9\%$ ) shift in  $\delta^{202}\text{Hg}$  compared to GEM.

Whereas  $\delta^{202}\text{Hg}$  tracks foliar uptake, the even isotope MIF signatures ( $\Delta^{200}\text{Hg}$  and  $\Delta^{204}\text{Hg}$ ) behave conservatively within the Pinet ecosystem and trace the different Hg wet and dry deposition sources to sphagnum. Sphagnum  $\Delta^{200}\text{Hg}$  and  $\Delta^{204}\text{Hg}$  ( $0.03 \pm 0.02$  and  $-0.04 \pm 0.04\%$ ) more closely resemble GEM  $\Delta^{200}\text{Hg}$  and  $\Delta^{204}\text{Hg}$  ( $-0.05 \pm 0.02$  and  $0.03 \pm 0.05\%$ ) than Hg wet deposition  $\Delta^{200}\text{Hg}$  and  $\Delta^{204}\text{Hg}$  ( $0.21 \pm 0.04$  and  $-0.31 \pm 0.10\%$ ) (Figure 2B and SI Figure S2B, Table S2). Similar to aspen foliage observations,<sup>39</sup> odd isotope MIF signatures in sphagnum may be affected by photochemical Hg reduction on wet sphagnum leaf and stem surfaces. We observe that sphagnum  $\Delta^{199}\text{Hg}$  and  $\Delta^{201}\text{Hg}$  ( $-0.11 \pm 0.09$  and  $-0.17 \pm 0.09\%$ ) closely track GEM  $\Delta^{199}\text{Hg}$  and  $\Delta^{201}\text{Hg}$  ( $-0.17 \pm 0.07$  and  $-0.16 \pm 0.08\%$ ), suggesting that  $\Delta^{199}\text{Hg}$  and  $\Delta^{201}\text{Hg}$  also predominantly reflect a GEM source. Photochemical foliar Hg reduction in sphagnum is however not negligible, based on small but significant differences between sphagnum vs GEM even and odd isotope MIF (see SI Figure S4). The combined GEM, wet deposition and sphagnum Hg isotope observations lead us to conclude that GEM dry deposition to sphagnum moss is the major pathway of atmospheric deposition to Pinet sphagnum. The Hg stable isotope signatures of pine needles, heather leaves and lichens collected at Pinet (SI Table S2, Figure 2) indicate a major contribution from GEM dry deposition as well.

**Hg Deposition Field Experiment.** Sphagnum moss grown under the opaque cover display similar Hg concentrations ( $49 \pm 14 \text{ ng g}^{-1}$ ,  $1\sigma$ ,  $n = 15$ ) as the adjacent uncovered control plot ( $39 \pm 7 \text{ ng g}^{-1}$ ,  $1\sigma$ ,  $n = 19$ ) (SI Figure S5), and with broadly similar  $\Delta^{199}\text{Hg}$ ,  $\Delta^{204}\text{Hg}$  ( $t$  test  $p > 0.05$ ), and  $\Delta^{200}\text{Hg}$ ,  $\Delta^{201}\text{Hg}$  (similar, though  $p < 0.05$ ) as atmospheric GEM (Figure 2 and SI Figure S2, Table S2). Among the five different Hg isotope signatures ( $\delta^{202}\text{Hg}$ ,  $\Delta^{199}\text{Hg}$ ,  $\Delta^{200}\text{Hg}$ ,  $\Delta^{201}\text{Hg}$ ,  $\Delta^{204}\text{Hg}$ ), all were significantly different from control to opaque-covered sphagnum (all  $t$  tests  $p < 0.05$ ). Glass-covered sphagnum also displays Hg stable isotope signatures distinct from control sphagnum ( $t$  tests  $p < 0.05$ , except for  $\Delta^{204}\text{Hg}$ ). These observations suggest that covering sphagnum with transparent or opaque surfaces affect sphagnum Hg isotope composition.

Control sphagnum shows higher  $\delta^{202}\text{Hg}$ ,  $\Delta^{199}\text{Hg}$ , and  $\Delta^{200}\text{Hg}$  compared to covered sphagnum (Figure 2 and SI Table S2). While  $\delta^{202}\text{Hg}$  and  $\Delta^{199}\text{Hg}$  signatures are potentially altered by photochemical processes, the difference in the conservative  $\Delta^{200}\text{Hg}$  signature indicates a lower contribution from Hg wet deposition in covered sphagnum plots, coherent with a reduction of rainfall due to the presence of a surface cover.

UV-radiation is known to induce photochemical odd isotope Hg MIF in aquatic systems<sup>20</sup> and possibly on wet vegetation.<sup>39</sup> A comparison between opaque and UV-transparent glass covered plots did not reveal significant differences in sphagnum  $\Delta^{199}\text{Hg}$  or  $\Delta^{201}\text{Hg}$  (nor  $\delta^{202}\text{Hg}$ ,  $\Delta^{200}\text{Hg}$ , and  $\Delta^{204}\text{Hg}$ , all  $t$  tests had  $p > 0.05$ ). Similar to our observations on control sphagnum plots,  $\Delta^{199}\text{Hg}$  of UV-transparent and opaque covered plots are  $0.1\%$  lower than expected from binary mixing between Hg wet deposition and GEM dry deposition (see SI Figure S4). This might indicate that while in-sphagnum Hg photoreduction occurs, incident light is not the limiting factor for this reaction.

Unlike previous studies on vascular plant foliage,<sup>42,43</sup> we did not find any strong seasonal variation in sphagnum Hg concentration (SI Table S2 and Figure S5). Seasonal variations in sphagnum Hg isotope composition were not observed for covered sphagnum either (glass or opaque, Figure 2 and SI Table S2). A comparison of control sphagnum collected during spring-summer times with fall-winter reveals some seasonal variations (SI Table S2,  $t$  test  $p < 0.05$  for  $\delta^{202}\text{Hg}$ ,  $\Delta^{199}\text{Hg}$ ,  $\Delta^{200}\text{Hg}$ , and  $\Delta^{201}\text{Hg}$ ). These differences seem to indicate a larger contribution of Hg wet deposition in the spring-summer period compared to fall-winter. The uptake of GEM by foliage is known to vary seasonally.<sup>14</sup> However, the growing period (spring-summer) is usually characterized by higher GEM uptake, which contrasts with our observations. Seasonal trends in Hg wet deposition have been reported as well, with higher Hg deposition in summer than in winter.<sup>44-46</sup> This could have caused the slightly higher sphagnum  $\Delta^{199}\text{Hg}$  and  $\Delta^{200}\text{Hg}$  in summer compared to winter.

Acrotelm and catotelm peat display similar odd ( $\Delta^{199}\text{Hg}$  of  $-0.19 \pm 0.05$  and  $-0.23 \pm 0.06\%$ ,  $1\sigma$ ,  $n = 12$  and  $22$  respectively) and even ( $\Delta^{200}\text{Hg}$  of  $0.01 \pm 0.04$  and  $0.00 \pm 0.04\%$  respectively) Hg isotope anomalies ( $t$  test  $p > 0.05$ , see SI Table S2). A significant difference in  $\delta^{202}\text{Hg}$  is however noted ( $-1.33 \pm 0.22\%$  for acrotelm and  $-1.49 \pm 0.14\%$  for catotelm peat,  $t$  test  $p < 0.05$ ), with catotelm peat slightly enriched in light Hg isotopes compared to acrotelm (SI Figure S6). Postdepositional processes were suggested to

modify peat Hg stable isotope composition,<sup>47</sup> with enrichment in heavy Hg isotopes caused by microbial reduction<sup>48</sup> or abiotic reduction by organic matter.<sup>22</sup> These reactions are however opposite to our observation of lower  $\delta^{202}\text{Hg}$  in more decomposed peat (SI Figure S6 and Table S2). Variations in  $\delta^{202}\text{Hg}$  can however be related to temporal changes in atmospheric Hg stable isotope signatures. We find that peat Hg isotope signatures (both acrotelm and catotelm) are similar to winter sphagnum ( $t$  test  $p > 0.05$  for  $\Delta^{199}\text{Hg}$ ,  $\Delta^{200}\text{Hg}$ ,  $\Delta^{201}\text{Hg}$ , and  $\Delta^{204}\text{Hg}$ ), probably because peat is formed by decomposition of sphagnum after senescence in winter.

**Hg Isotope Mass Balance.** We use a binary isotope mixing model based on the conservative  $\Delta^{200}\text{Hg}$  and  $\Delta^{204}\text{Hg}$  signatures (see SI) to calculate that  $21 \pm 9\%$  ( $7.0 \pm 3.3 \mu\text{g m}^{-2} \text{y}^{-1}$ ) of net Hg accumulation by sphagnum (control plots, winter time) is from Hg wet deposition and  $79 \pm 9\%$  ( $27 \pm 13 \mu\text{g m}^{-2} \text{y}^{-1}$ ) from GEM dry deposition (Figure 3). The former is compatible with measured Hg wet deposition of  $9 \mu\text{g m}^{-2} \text{y}^{-1}$  at Pinet (Table 1). Such low contribution from Hg wet deposition is consistent with an estimated 16% contribution of rainfall Hg to forest floor Hg in the aspen study,<sup>39</sup> and about 33% in a subalpine grassland (and 67% for GEM dry deposition, corresponding to more than  $20 \mu\text{g m}^{-2} \text{y}^{-1}$ ).<sup>36</sup> The consistency we find between the mass balances based on Hg deposition and on Hg stable isotopes argue against a large overestimation of HgAR due to inaccurate  $^{210}\text{Pb}$  dating.<sup>32,33</sup> Slightly higher GEM dry deposition contributions of  $88 \pm 7\%$  and  $83 \pm 8\%$  are found for opaque and glass-covered sphagnum, respectively.

The substantial dry deposition of GEM that we infer from the  $\Delta^{200}\text{Hg}$  and  $\Delta^{204}\text{Hg}$  isotope mixing models is also reflected in ambient GEM concentrations and GEM  $\delta^{202}\text{Hg}$  at the Pinet peat bog. Mean GEM concentration at Pinet ( $1.2 \pm 0.2 \text{ ng m}^{-3}$ ,  $1\sigma$ ,  $n = 10$ ) is significantly lower than the regional background GEM level in the Pyrenees Mountains, as observed at the nearby Pic du Midi ( $1.5 \pm 0.3 \text{ ng m}^{-3}$ ) and 14 other European sites (median GEM of  $1.7 \text{ ng m}^{-3}$ ).<sup>27</sup> Pinet GEM  $\delta^{202}\text{Hg}$  of 1.2‰ is significantly enriched in the heavier Hg isotopes compared to Pic du Midi GEM  $\delta^{202}\text{Hg}$  of 0.6‰. Similar trends were observed in the Rhineland aspen forest, with low total gaseous Hg (TGM  $\sim$  GEM) levels of  $1.0 \text{ ng m}^{-3}$  and elevated TGM  $\delta^{202}\text{Hg}$  up to 0.93‰.<sup>39</sup> We use a Rayleigh fractionation model (see SI Figure S7) to calculate that a  $0.3 \text{ ng m}^{-3}$  decline ( $1.5\text{--}1.2 \text{ ng m}^{-3}$ ) in GEM concentration at Pinet with an associated 0.6‰ increase (0.6–1.2‰) in GEM  $\delta^{202}\text{Hg}$  due to regional GEM dry deposition requires an isotope fractionation factor of  $-2.6\%$ . This fractionation factor is compatible with the observed Hg isotope fractionation between ambient GEM  $\delta^{202}\text{Hg}$  and sphagnum, pine needles, *calluna* leaves and lichens at the Pinet bog ( $-2.3$  to  $-2.8\%$ ), and with aspen leaves at the Rhineland aspen forest ( $-2.9\%$ ).<sup>39</sup> These coherent GEM and vegetation Hg concentration and isotope signatures imply that GEM dry deposition to vegetation is capable of substantially drawing down atmospheric GEM levels and reducing the atmospheric GEM lifetime. Such interaction between atmosphere and vegetation is supported also by strong spatial gradients in GEM across forests.<sup>42</sup> GEM concentration in a maple forest ( $1.4 \text{ ng m}^{-3}$ ) was found to be  $0.4 \text{ ng m}^{-3}$  lower than at an adjacent (300 m) open area ( $1.0 \text{ ng m}^{-3}$ ).<sup>42</sup> Together with GEM flux measurements over vegetation,<sup>17</sup> we therefore suggest that vegetated ecosystems are a net sink for atmospheric GEM.

**Implications.** Our findings suggest that the ombrotrophic Pinet peat deposit records predominantly atmospheric GEM dry deposition, rather than Hg wet deposition. Variations in past HgAR inferred from ombrotrophic peat records thus represent mainly variations in local GEM concentration. GEM dry deposition velocity may however be strongly affected by local vegetation and changes therein, impacting GEM uptake and therefore HgARs.<sup>49</sup> Such dependence of peat HgAR on vegetation would explain the commonly observed large variability in peat HgAR within a single peat bog.<sup>50–52</sup> Elevated HgAR in peat bogs, as compared to Hg wet deposition, has previously been attributed to bias in the  $^{210}\text{Pb}$  chronometer due to  $^{210}\text{Pb}$  mobility.<sup>32,33</sup> Our findings suggest that elevated HgAR are essentially due to the overlooked GEM dry deposition flux.

Lake sediments have been extensively used as natural archives of atmospheric Hg deposition.<sup>32,53–55</sup> Lake sediments integrate Hg wet and dry deposition to the lake surface but also to the larger surrounding watershed. The average  $\Delta^{199}\text{Hg}$  and  $\Delta^{200}\text{Hg}$  found in freshwater surface sediments are  $-0.03 \pm 0.13\%$  ( $1\sigma$ ,  $n = 371$ ) and  $0.02 \pm 0.06\%$  ( $1\sigma$ ,  $n = 306$ )<sup>19</sup> respectively, and contrast with global Hg rainfall observations which display positive  $\Delta^{199}\text{Hg}$  ( $0.37 \pm 0.25\%$ ,  $1\sigma$ ,  $n = 105$ ) and  $\Delta^{200}\text{Hg}$  ( $0.18 \pm 0.15\%$ ,  $1\sigma$ ,  $n = 105$ ). As observed for the Pinet bog, a significant fraction of Hg deposited to lake sediments may therefore ultimately also derive from GEM dry deposition to vegetation and soils of the lake watershed, which is then transferred to the lake.<sup>56</sup>  $\Delta^{200}\text{Hg}$  mass balance using the above global rainfall end-member and global GEM end-member ( $\Delta^{200}\text{Hg} = -0.05 \pm 0.04\%$ ,  $1\sigma$ ,  $n = 69$ ) suggests that  $63 \pm 28\%$  ( $1\sigma$ ) of freshwater sediment Hg is derived from GEM dry deposition to the watershed. The contribution of GEM dry deposition to freshwater sediments however likely depends on watershed characteristics (size, erosion, water flow), as suggested by the large variability we infer from the mass balance approach ( $1\sigma = 28\%$ ).

Globally, most terrestrial samples (soils, foliage, litter, lichens) display negative  $\delta^{202}\text{Hg}$  ( $-1.3 \pm 0.8\%$ ,  $1\sigma$ ,  $n = 162$ ) and  $\Delta^{199}\text{Hg}$  ( $-0.2 \pm 0.2\%$ ,  $1\sigma$ ,  $n = 163$ ), and insignificant  $\Delta^{200}\text{Hg}$  ( $0.03 \pm 0.04\%$ ,  $1\sigma$ ,  $n = 119$ ),<sup>19</sup> similar to our observations on sphagnum moss and peat. This further supports the idea that modern Hg deposition to vegetated ecosystems is dominated by GEM dry deposition. A global GEM dry deposition flux to continents that is three times larger than wet deposition results in a reduced lifetime of atmospheric GEM. A crude approximation of this effect can be calculated from global Hg mass budget and flux estimates of  $5600 \text{ Mg}$  (atmosphere),  $1600 \text{ Mg y}^{-1}$  (GEM dry deposition to continents),  $2600 \text{ mg y}^{-1}$  ( $\text{Hg}^{\text{II}}$  deposition to continents),  $7100 \text{ Mg y}^{-1}$  (Hg deposition to oceans), and associated lifetime of 0.5 years.<sup>6</sup> Increasing GEM dry deposition to  $3\times$  the well-constrained Hg wet deposition (to continents) value lowers the GEM lifetime to 0.33 years (4 months), which is consistent with lower bound estimates from global Hg models.<sup>57</sup> Deforestation by human activities over millennia has decreased global forest covered area by 50%<sup>58</sup> and therefore possibly affected global Hg cycling by reducing GEM exchanges between foliage and the atmosphere. Future archive and modeling studies should therefore explore the link between regional and global vegetation changes to HgAR.

## AUTHOR INFORMATION

### Corresponding Authors

\*(M.E.) Phone: +33 5 61 33 26 06 e-mail: [maxime.enrico@get.obs-mip.fr](mailto:maxime.enrico@get.obs-mip.fr).

\*(J.E.S.) E-mail: [sonke@get.obs-mip.fr](mailto:sonke@get.obs-mip.fr).

### Present Addresses

§(L-E.H.) University of Aix-Marseille, Mediterranean Institute of Oceanography (MIO), 163 Avenue de Luminy, 13288 Marseille, France.

<sup>1</sup>(X.F.) State Key Laboratory of Environmental Geochemistry, Institute of Geochemistry, Chinese Academy of Sciences, Guiyang, China.

#(R.S.) CAS Key Laboratory of Crust-Mantle Materials and Environment, School of Earth and Space Sciences, University of Science and Technology of China, Hefei 230026, China.

### Notes

The authors declare no competing financial interest.

## ACKNOWLEDGMENTS

This work was supported by research grants ANR-09-JCJC-0035-01 from the French Agence Nationale de Recherche and ERC-2010-StG\_20091028 from the European Research Council to JES. Bruno Le Roux and the Association Aude Claire are thanked for Pinet coring permission and help on the field. We thank Pieter Van Beek and Marc Souhaut from LAFARA for radionuclides measurements, Jérôme Chmeleff for ICP-MS maintenance, and the Pic du Midi tech team for logistical support. Laura Sherman is thanked for providing a rainwater Hg preconcentration protocol, and Chris Holmes is thanked for providing EMEP rainfall Hg data.

## REFERENCES

- (1) Mergler, D.; Anderson, H. A.; Chan, L. H.; Mahaffey, K. R.; Murray, M.; Sakamoto, M.; Stern, A. H. Methylmercury exposure and health effects in humans: a worldwide concern. *Ambio* **2007**, *36* (1), 3–11.
- (2) Zhang, Y.; Jacob, D. J.; Horowitz, H. M.; Chen, L.; Amos, H. M.; Krabbenhoft, D. P.; Slemr, F.; St. Louis, V. L.; Sunderland, E. M. Observed decrease in atmospheric mercury explained by global decline in anthropogenic emissions. *Proc. Natl. Acad. Sci. U. S. A.* **2016**, *113* (3), 526–531.
- (3) Bagnato, E.; Tamburello, G.; Avard, G.; Martinez-Cruz, M.; Enrico, M.; Fu, X.; Sprovieri, M.; Sonke, J. E. *Mercury Fluxes from Volcanic and Geothermal Sources: An Update*, Special Publications; Geological Society: London, 2014; Vol. 410, (1), 263–285.
- (4) Amos, H. M.; Sonke, J. E.; Obrist, D.; Robins, N.; Hagan, N.; Horowitz, H. M.; Mason, R. P.; Witt, M.; Hedgcock, I. M.; Corbitt, E. S.; Sunderland, E. M. Observational and modeling constraints on global anthropogenic enrichment of mercury. *Environ. Sci. Technol.* **2015**, *49* (7), 4036–47.
- (5) *Global Mercury Assessment t2013: Sources, Emissions, Releases and Environmental Transport*; UNEP Chemicals Branch: Geneva, Switzerland, 2013; <http://www.unep.org/PDF/PressReleases/GlobalMercuryAssessment2013.pdf>.
- (6) Selin, N. E.; Jacob, D. J.; Yantosca, R. M.; Strode, S.; Jaeglé, L.; Sunderland, E. M. Global 3-D land-ocean-atmosphere model for mercury: Present-day versus preindustrial cycles and anthropogenic

enrichment factors for deposition. *Global Biogeochemical Cycles* **2008**, *22* (2), GB2011.

(7) Lindberg, S.; Bullock, R.; Ebinghaus, R.; Engstrom, D.; Feng, X. B.; Fitzgerald, W.; Pirrone, N.; Prestbo, E.; Seigneur, C. A synthesis of progress and uncertainties in attributing the sources of mercury in deposition. *Ambio* **2007**, *36* (1), 19–32.

(8) Gustin, M. S., Exchange of mercury between the atmosphere and terrestrial ecosystems. In *Environmental Chemistry and Toxicology of Mercury*; John Wiley & Sons, Inc., 2011; pp 423–451.

(9) Hanson, P. J.; Lindberg, S. E.; Tabberer, T. A.; Owens, J. G.; Kim, K. H. Foliar exchange of mercury vapor: Evidence for a compensation point. *Water, Air, Soil Pollut.* **1995**, *80* (1–4), 373–382.

(10) Zhang, L. M.; Wright, L. P.; Blanchard, P. A review of current knowledge concerning dry deposition of atmospheric mercury. *Atmos. Environ.* **2009**, *43* (37), 5853–5864.

(11) Erickson, J. A.; Gustin, M. S. Foliar exchange of mercury as a function of soil and air mercury concentrations. *Sci. Total Environ.* **2004**, *324* (1–3), 271–9.

(12) Wright, L. P.; Zhang, L. An approach estimating bidirectional air-surface exchange for gaseous elemental mercury at AMNet sites. *J. Adv. Model. Earth Syst.* **2015**, *7* (1), 35–49.

(13) Obrist, D.; Johnson, D. W.; Edmonds, R. L. Effects of vegetation type on mercury concentrations and pools in two adjacent coniferous and deciduous forests. *J. Plant Nutr. Soil Sci.* **2012**, *175* (1), 68–77.

(14) Converse, A. D.; Riscassi, A. L.; Scanlon, T. M. Seasonal variability in gaseous mercury fluxes measured in a high-elevation meadow. *Atmos. Environ.* **2010**, *44* (18), 2176–2185.

(15) Gustin, M. S.; Taylor, G. E.; Maxey, R. A. Effect of temperature and air movement on the flux of elemental mercury from substrate to the atmosphere. *Journal of Geophysical Research: Atmospheres* **1997**, *102* (D3), 3891–3898.

(16) Gustin, M. S.; Lindberg, S. E.; Weisberg, P. J. An update on the natural sources and sinks of atmospheric mercury. *Appl. Geochem.* **2008**, *23* (3), 482–493.

(17) Agnan, Y.; Le Dantec, T.; Moore, C. W.; Edwards, G. C.; Obrist, D. New Constraints on Terrestrial Surface-Atmosphere Fluxes of Gaseous Elemental Mercury Using a Global Database. *Environ. Sci. Technol.* **2016**, *50* (2), 507–24.

(18) Bergquist, R. A.; Blum, J. D. The Odds and Evens of Mercury Isotopes: Applications of Mass-Dependent and Mass-Independent Isotope Fractionation. *Elements* **2009**, *5* (6), 353–357.

(19) Blum, J. D.; Sherman, L. S.; Johnson, M. W. Mercury Isotopes in Earth and Environmental Sciences. *Annu. Rev. Earth Planet. Sci.* **2014**, *42* (1), 249–269.

(20) Bergquist, B. A.; Blum, J. D. Mass-Dependent and -Independent Fractionation of Hg Isotopes by Photoreduction in Aquatic Systems. *Science* **2007**, *318* (5849), 417–420.

(21) Estrade, N.; Carignan, J.; Sonke, J. E.; Donard, O. F. X. Mercury isotope fractionation during liquid-vapor evaporation experiments. *Geochim. Cosmochim. Acta* **2009**, *73* (10), 2693–2711.

(22) Zheng, W.; Hintelmann, H. Nuclear field shift effect in isotope fractionation of mercury during abiotic reduction in the absence of light. *J. Phys. Chem. A* **2010**, *114* (12), 4238–45.

(23) Gratz, L. E.; Keeler, G. J.; Blum, J. D.; Sherman, L. S. Isotopic composition and fractionation of mercury in Great Lakes precipitation and ambient air. *Environ. Sci. Technol.* **2010**, *44* (20), 7764–70.

(24) Chen, J. B.; Hintelmann, H.; Feng, X. B.; Dimock, B. Unusual fractionation of both odd and even mercury isotopes in precipitation from Peterborough, ON, Canada. *Geochim. Cosmochim. Acta* **2012**, *90* (0), 33–46.

(25) Fu, X. W.; Heimbürger, L. E.; Sonke, J. E. Collection of atmospheric gaseous mercury for stable isotope analysis using iodine- and chlorine-impregnated activated carbon traps. *J. Anal. At. Spectrom.* **2014**, *29* (5), 841–852.

(26) Huang, J.; Miller, M. B.; Weiss-Penzias, P.; Gustin, M. S. Comparison of gaseous oxidized Hg measured by KCl-coated denuders, and nylon and cation exchange membranes. *Environ. Sci. Technol.* **2013**, *47* (13), 7307–16.



- (27) Sprovieri, F.; Pirrone, N.; Ebinghaus, R.; Kock, H.; Dommergue, A. A review of worldwide atmospheric mercury measurements. *Atmos. Chem. Phys.* **2010**, *10* (17), 8245–8265.
- (28) Sun, R.; Enrico, M.; Heimbürger, L. E.; Scott, C.; Sonke, J. E. A double-stage tube furnace–acid-trapping protocol for the pre-concentration of mercury from solid samples for isotopic analysis. *Anal. Bioanal. Chem.* **2013**, *405* (21), 6771–81.
- (29) Sherman, L. S.; Blum, J. D.; Keeler, G. J.; Demers, J. D.; Dvonch, J. T. Investigation of local mercury deposition from a coal-fired power plant using mercury isotopes. *Environ. Sci. Technol.* **2012**, *46* (1), 382–90.
- (30) European Monitoring and Evaluation Programme (EMEP) Website. <http://www.emep.int/>.
- (31) National Atmospheric Deposition Program - Mercury deposition Network (NADP-MDN) Website. <http://nadp.sws.uiuc.edu/mdn/>.
- (32) Biester, H.; Bindler, R.; Martinez-Cortizas, A.; Engstrom, D. R. Modeling the past atmospheric deposition of mercury using natural archives. *Environ. Sci. Technol.* **2007**, *41* (14), 4851–4860.
- (33) Hansson, S. V.; Kaste, J. M.; Olid, C.; Bindler, R. Incorporation of radiometric tracers in peat and implications for estimating accumulation rates. *Sci. Total Environ.* **2014**, *493* (0), 170–7.
- (34) Lan, X.; Talbot, R.; Castro, M.; Perry, K.; Luke, W. Seasonal and diurnal variations of atmospheric mercury across the US determined from AMNet monitoring data. *Atmos. Chem. Phys.* **2012**, *12* (21), 10569–10582.
- (35) Amos, H. M.; Jacob, D. J.; Holmes, C. D.; Fisher, J. A.; Wang, Q.; Yantosca, R. M.; Corbitt, E. S.; Galarneau, E.; Rutter, A. P.; Gustin, M. S.; Steffen, A.; Schauer, J. J.; Graydon, J. A.; Louis, V. L., St; Talbot, R. W.; Edgerton, E. S.; Zhang, Y.; Sunderland, E. M. Gas-particle partitioning of atmospheric Hg(II) and its effect on global mercury deposition. *Atmos. Chem. Phys.* **2012**, *12* (1), 591–603.
- (36) Fritsche, J.; Obrist, D.; Zeeman, M. J.; Conen, F.; Eugster, W.; Alewell, C. Elemental mercury fluxes over a sub-alpine grassland determined with two micrometeorological methods. *Atmos. Environ.* **2008**, *42* (13), 2922–2933.
- (37) Fu, X.; Feng, X.; Sommar, J.; Wang, S. A review of studies on atmospheric mercury in China. *Sci. Total Environ.* **2012**, *421–422*, 73–81.
- (38) Risch, M. R.; DeWild, J. F.; Krabbenhoft, D. P.; Kolka, R. K.; Zhang, L. Litterfall mercury dry deposition in the eastern USA. *Environ. Pollut.* **2012**, *161*, 284–290.
- (39) Demers, J. D.; Blum, J. D.; Zak, D. R. Mercury isotopes in a forested ecosystem: Implications for air-surface exchange dynamics and the global mercury cycle. *Global Biogeochemical Cycles* **2013**, *27* (1), 222–238.
- (40) Demers, J. D.; Sherman, L. S.; Blum, J. D.; Marsik, F. J.; Dvonch, J. T. Coupling atmospheric mercury isotope ratios and meteorology to identify sources of mercury impacting a coastal urban-industrial region near Pensacola, Florida, USA. *Global Biogeochemical Cycles* **2015**, *29* (10), 1689–1705.
- (41) Wang, Z.; Chen, J.; Feng, X.; Hintelmann, H.; Yuan, S.; Cai, H.; Huang, Q.; Wang, S.; Wang, F. Mass-dependent and mass-independent fractionation of mercury isotopes in precipitation from Guiyang, SW China. *C. R. Geosci.* **2015**, *347* (7–8), 358–367.
- (42) Poissant, L.; Pilote, M.; Yumvihoze, E.; Lean, D. Mercury concentrations and foliage/atmosphere fluxes in a maple forest ecosystem in Québec, Canada. *J. Geophys. Res.* **2008**, *113* (D10), D10307.
- (43) Rea, A. W.; Lindberg, S. E.; Scherbatskoy, T.; Keeler, G. J. Mercury Accumulation in Foliage over Time in Two Northern Mixed-Hardwood Forests. *Water, Air, Soil Pollut.* **2002**, *133* (1–4), 49–67.
- (44) Prestbo, E. M.; Gay, D. A. Wet deposition of mercury in the U.S. and Canada, 1996–2005: Results and analysis of the NADP mercury deposition network (MDN). *Atmos. Environ.* **2009**, *43* (27), 4223–4233.
- (45) Mason, R. P.; Lawson, N. M.; Sheu, G. R. Annual and seasonal trends in mercury deposition in Maryland. *Atmos. Environ.* **2000**, *34* (11), 1691–1701.
- (46) Selin, N. E.; Jacob, D. J. Seasonal and spatial patterns of mercury wet deposition in the United States: Constraints on the contribution from North American anthropogenic sources. *Atmos. Environ.* **2008**, *42* (21), 5193–5204.
- (47) Jiskra, M.; Wiederhold, J. G.; Skyllberg, U.; Kronberg, R. M.; Hajdas, I.; Kretzschmar, R. Mercury deposition and re-emission pathways in boreal forest soils investigated with Hg isotope signatures. *Environ. Sci. Technol.* **2015**, *49* (12), 7188–96.
- (48) Kritee, K.; Blum, J. D.; Johnson, M. W.; Bergquist, B. A.; Barkay, T. Mercury stable isotope fractionation during reduction of Hg(II) to Hg(0) by mercury resistant microorganisms. *Environ. Sci. Technol.* **2007**, *41* (6), 1889–95.
- (49) Outridge, P. M.; Sanei, H. Does organic matter degradation affect the reconstruction of pre-industrial atmospheric mercury deposition rates from peat cores? — A test of the hypothesis using a permafrost peat deposit in northern Canada. *Int. J. Coal Geol.* **2010**, *83* (1), 73–81.
- (50) Martínez Cortizas, A.; Peiteado Varela, E.; Bindler, R.; Biester, H.; Cheburkin, A. Reconstructing historical Pb and Hg pollution in NW Spain using multiple cores from the Chao de Lamoso bog (Xistral Mountains). *Geochim. Cosmochim. Acta* **2012**, *82* (0), 68–78.
- (51) Bindler, R.; Klarqvist, M.; Klaminder, J.; Förster, J. Does within-bog spatial variability of mercury and lead constrain reconstructions of absolute deposition rates from single peat records? The example of Store Mosse, Sweden. *Global Biogeochemical Cycles* **2004**, *18* (3), GB3020.
- (52) Rydberg, J.; Karlsson, J.; Nyman, R.; Wanhatola, I.; Nathe, K.; Bindler, R. Importance of vegetation type for mercury sequestration in the northern Swedish mire, Rodmossamyran. *Geochim. Cosmochim. Acta* **2010**, *74* (24), 7116–7126.
- (53) Zhang, Y.; Jaeglé, L.; Thompson, L.; Streets, D. G. Six centuries of changing oceanic mercury. *Global Biogeochemical Cycles* **2014**, *28* (11), 2014GB004939.
- (54) Engstrom, D. R.; Fitzgerald, W. F.; Cooke, C. A.; Lamborg, C. H.; Drevnick, P. E.; Swain, E. B.; Balogh, S. J.; Balcom, P. H. Atmospheric Hg emissions from preindustrial gold and silver extraction in the Americas: a reevaluation from lake-sediment archives. *Environ. Sci. Technol.* **2014**, *48* (12), 6533–43.
- (55) Fitzgerald, W. F.; Engstrom, D. R.; Lamborg, C. H.; Tseng, C.-M.; Balcom, P. H.; Hammerschmidt, C. R. Modern and Historic Atmospheric Mercury Fluxes in Northern Alaska: Global Sources and Arctic Depletion. *Environ. Sci. Technol.* **2005**, *39* (2), 557–568.
- (56) Rydberg, J.; Rösch, M.; Heinz, E.; Biester, H. Influence of catchment vegetation on mercury accumulation in lake sediments from a long-term perspective. *Sci. Total Environ.* **2015**, *538*, 896–904.
- (57) Parrella, J. P.; Jacob, D. J.; Liang, Q.; Zhang, Y.; Mickley, L. J.; Miller, B.; Evans, M. J.; Yang, X.; Pyle, J. A.; Theys, N.; Van Roozendaal, M. Tropospheric bromine chemistry: implications for present and pre-industrial ozone and mercury. *Atmos. Chem. Phys.* **2012**, *12* (15), 6723–6740.
- (58) Kaplan, J. O.; Krumhardt, K. M.; Zimmermann, N. The prehistoric and preindustrial deforestation of Europe. *Quat. Sci. Rev.* **2009**, *28* (27–28), 3016–3034.